Journal of Marine Research, 56, 239–255, 1998

Under-ice observations of water column temperature, salinity and spring phytoplankton dynamics: Eastern Bering Sea shelf

by P. J. Stabeno[1], J. D. Schumacher[1], R. F. Davis[2] and J. M. Napp[3]

ABSTRACT

The inundation of two moored platforms by sea ice in late winter and early spring of 1995 provided unique time series of water column temperature, salinity, estimated chlorophyll-*a*, and phytoplankton fluorescence under advancing and retreating sea ice. One platform was located at 72 m in the weakly advective middle shelf regime. Here, chlorophyll-*a* concentrations began increasing shortly after the arrival of the ice (March) during the period of weak stratification and continued to increase while wind actively mixed the water column to >60 m. Changes in water column structure and properties resulted from an event of strong advection rather than vertical fluxes. During winter, such advective events can replenish the nutrients required to support the rich blooms that occur over the middle shelf during spring. The advancing ice was associated with the coldest waters and a deep (>50 m) mixed layer. The ice melt enhanced the two-layer system previously established by advection. A second mooring was located at the 120 m isobath on the more advective outer shelf. The ice reached this site on April 6, and chlorophyll-*a* concentrations increased as the sea ice melted. At the third mooring, located on the shelf farther south beyond the range of ice, the spring bloom began on ~May 9.

1. Introduction

In March 1995 three surface moorings with accompanying acoustic Doppler current profilers (ADCPs) were deployed on the southeastern Bering Sea shelf (Fig. 1) as part of an experiment conducted by Fisheries Oceanography Coordinated Investigations for NOAA's Coastal Ocean Program. The purpose of this experiment was to obtain time series of physical and biological variables to characterize the changing nature of the shelf waters in spring and summer. Surface floats supported instruments that measured a variety of atmospheric variables. Subsurface instruments measured temperature and conductivity (salinity), phytoplankton fluorescence, and chlorophyll-*a* absorbance. The nearby ADCPs provided time series of currents through most of the water column.

While it has long been desirable to measure a suite of oceanographic parameters under an advancing ice field, this experiment was not designed to accomplish this. On March 17,

1. NOAA, Pacific Marine Environmental Laboratory, 7600 Sand Point Way NE, Seattle, Washington, 98115, U.S.A.
2. Department of Oceanography, Dalhousie University, Nova Scotia, Canada.
3. NOAA, Alaska Fisheries Science Center, 7600 Sand Point Way NE, Seattle, Washington, 98115, U.S.A.

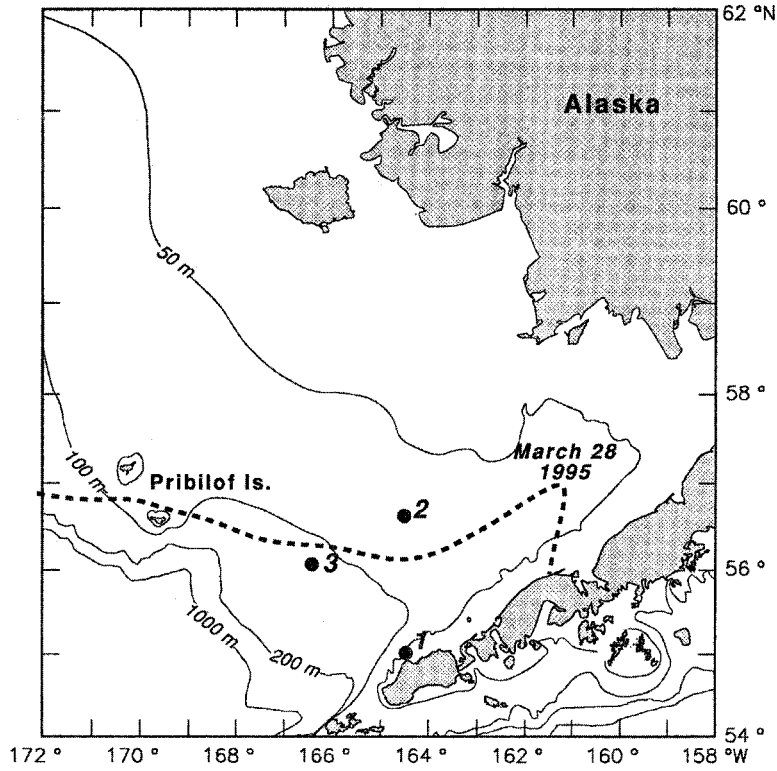

Figure 1. A map of the eastern Bering Sea continental shelf indicating the locations of the three moorings. Maximum ice extent during 1995 is shown by a dashed line. Depth contours are in meters.

a period of steady winds out of the north pushed the ice ~100 km southward in ~2 days (Fig. 2). The ice reached mooring 2 three days after deployment and dragged the mooring ~9 km southward. We continued to obtain position fixes via Service Argos for ~9 days. Mooring 3 met a similar fate on April 8, when it was dragged 2 km southward by the advancing ice. The ice continued southward, and at its maximum extent, mooring 2 was >100 km from the ice edge. In contrast, mooring 3 remained near the ice edge (within 10 km) until the ice retreated on ~April 20. The ice did not reach the southernmost mooring.

On April 29 the NOAA ship *Miller Freeman* found and recovered mooring 2, ~14 km south of its deployment site. The surface buoy was badly damaged (approximately two-thirds of the foam had been rubbed away by the ice) and stripped of all meteorological sensors. Six days later, mooring 3 was found and recovered ~5 km south of its deployment site. This surface buoy was in slightly better condition, but all surface instruments had been damaged. On both moorings, however, the subsurface instruments escaped damage by ice and provided unique time series of temperature, salinity, and chlorophyll-*a* estimates underneath an advancing and retreating ice field.

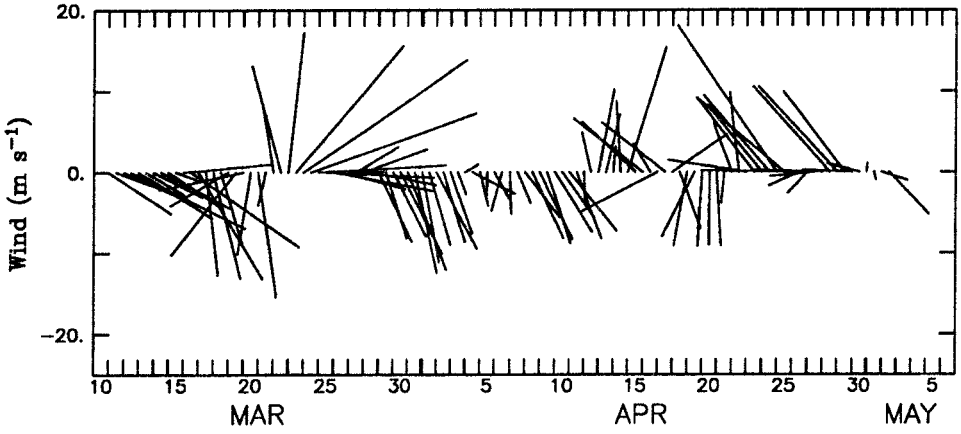

Figure 2. Wind velocity derived from atmospheric pressure and interpolated to a point midway between moorings 1 and 2. North is along the y-axis.

This paper focuses on the observations from the two sites that were within the ice field. In the next section we give a brief background of the region and then describe the mooring design, instruments, and data processing. The time series of temperature and salinity, currents, shear, and chlorophyll-*a* are presented in the following sections. We close with a discussion of the conclusions derived from this data set.

2. Background

The eastern Bering Sea covers a broad (>500 km), shallow continental shelf. The shelf is divided into three depth domains, coastal (0-50 m), middle (50-100 m), and outer (100-180 m), with distinctive hydrographic, circulation, and planktonic community characteristics (Cooney and Coyle, 1982; Coachman, 1986; Walsh and McRoy, 1986; Schumacher and Stabeno, 1998). During spring-summer, the hydrographic domains exhibit distinct vertical structure: well mixed or weakly stratified in the coastal domain; strongly two-layered over the middle shelf; and upper and lower-mixed layers separated by a region with fine structure on the outer shelf. Mooring 2 was deployed in the middle domain to measure biophysical variables during the evolution of the two-layer system during spring and summer; mooring 3 was positioned to measure changes in the more oceanic character of the outer shelf. Mooring 1 was deployed near the Alaskan Peninsula, in a region influenced by water from Alaska Coastal Current advected through Unimak Pass and slope water advected up Bering Canyon.

The eastern Bering Sea shelf is a marginal ice zone where polar and subarctic systems interact. During the summer and fall the shelf is usually ice free. In winter the juxtaposition of the Aleutian Low and Siberian High results in strong, frigid winter winds from the northeast. These winds cause extensive ice formation along leeward coasts, which is then advected southwestward. The leading edge of the ice is continuously melting, introducing

cold, freshwater to the water column. Maximum ice extent is typically in late March (Wyllie-Echeverria, 1995). The location of the southernmost position of the ice varies over hundreds of kilometers. In extreme years (e.g., 1976), ice covers the entire southeastern shelf (Fig. 1). The extent of the ice influences the temperature and horizontal extent of a cold pool that occurs in the lower layer of the middle shelf. The cold pool, which is 40-50 m thick, persists through the summer, warming only slightly (often $<2°C$).

The eastern Bering Sea shelf is one of the most productive regions of the world's oceans (Walsh and McRoy, 1986). Ice-edge phytoplankton blooms are common features in marginal ice zones during the spring (Smith, 1987; Niebauer, 1991) and produce a large fraction of the annual primary production over the shelf. This occurs as the ice melts back in the spring and a surface mixed layer is formed as a result of the increase in freshwater (Niebauer *et al.,* 1995). The rapid increase in chlorophyll can be assisted by the seeding of the water column with ice algae (Schandelmeier and Alexander, 1981).

3. Methods

a. Shipboard measurements

Immediately following deployment and before recovery of each mooring, a conductivity-temperature-depth (CTD) cast with Niskin bottles was done at each site. Discrete water samples for determination of chlorophyll-*a*, pheophytin-*a*, and nutrients were obtained in the vicinity of the moorings. Aliquots of seawater were filtered through Whatman GF/F filters and stored at $-70°C$ until 24-hr cold extraction in 90% acetone and fluorometric analysis could be performed (Parsons *et al.,* 1984). Nutrient samples were frozen for later colorometric analysis (Whitledge *et al.,* 1981).

b. Surface moorings

The surface moorings consisted of chains supported by a surface toroid. The length of the tether was $\sim$50% longer than the water depths, permitting horizontal motion. The mooring float was a 2.3-m-diameter foam-filled fiberglass toroid with a rigid 2-m-long bridle. The meteorological instruments were mounted on a 3.5-m aluminum tower. Oceanographic instruments were mounted on the buoys' bridle and mooring lines. SBE 16-03 SEACATs recorded temperature, conductivity (salinity), and usually pressure, to accuracies of 0.01°C, 0.001 practical salinity units (psu), and 0.14 decibar (db), respectively. Temperature was also recorded by miniature temperature recorders (MTR). Chlorophyll absorption meters were on each mooring and, in addition, fluorometers were used on mooring 2 in conjunction with the SEACATs. The positions of all equipment on each mooring are provided in Table 1. Two of the SEACATs (11 and 22 m) flooded due to failure of the O-rings, likely caused by going from the cold temperature on deck to the relatively warm water ($\sim$0.5°C). In addition, the chlorophyll absorption meter at 14 m on mooring 2 ceased functioning on March 25, and the data are not presented.

Most instruments were calibrated before deployment and after recovery. The time base

Table 1. Mooring location, water depth, deployment period, and depths (m) of subsurface instruments. ADCPs (with SEACAT[1]) were deployed within 1 km of surface mooring. Instruments that failed and provided no data are indicated by asterisks (*).

	MTR	SEACAT	Fluorometer	A-3
Mooring 1	1			
55°04′:164°31′	15	10		5*
65 m	20	26		21
March 14–June 15	32	44		
600 KHz ADCP	38	60[1]		
	50			
Mooring 2	1			
56°36′:164°37′	15	11*	11*	7
75 m	20	22*	22*	14*
March 14–April 29	32	44	44	
150 KHz ADCP	38	68[1]		
	50			
	56			
Mooring 3	1	10		7
56°02′:166°23′	15	26		
123 m	20	44		
March 13–May 8	32	80		
150 KHz ADCP	38	118[1]		
	50			
	56			

was adjusted, if necessary, following checks for missing records and clock drift. Spikes were removed from the time series. These were most common in the salinity time series due to the different response times of the temperature and conductivity sensor.

The chlorophyll-*a* absorption meters were A-3s from Western Environmental Technology Laboratories and measured in situ absorption at 650, 676, and 710 nm. Long-term deployment of these instruments is described in some detail in Davis *et al.* (1997). Absorption values were converted into estimates of chlorophyll-*a* concentration using standard spectrophotometric techniques (Parsons *et al.,* 1984) and a constant chlorophyll absorption coefficient of 0.017 m^2 (mg chl)$^{-1}$ (Davis *et al.,* 1997). Simulated chlorophyll fluorescence was measured using WET Lab's Wet Star fluorometers. *In situ* fluorescence was converted to chlorophyll-*a* concentration using instrument-specific empirical relationships determined in the laboratory at two temperatures using cultured phytoplankton.

c. Acoustic Doppler Current Profiler

A 150-KHz ADCP was deployed at mooring sites 2 and 3, and a 600-KHz ADCP at site 1. The extensive fishing in this region necessitated the use of trawl-resistant cages (TRAP). Each TRAP is a five-sided structure approximately 3.5 m in diameter and 0.8 m tall. Each contained an upward-looking ADCP with a 90° head, an external alkaline battery pack, two recovery floats with 400 m of line attached to each, and two releases. In addition, one

SEACAT with a 5-m-long tube was positioned in the cage to measure temperature and salinity at 5 m above the bottom.

The 150-KHz (600-KHz) ADCP measured averaged velocities at half-hour intervals in 4-m (2-m) bins. The time series of currents presented in this paper have been low pass filtered with a 35-hour, cosine-squared, tapered Lanczos filter to remove high-frequency variability (especially the diurnal and semi-diurnal tidal signals), and then resampled at 6-hour intervals.

d. Winds

Since no winds were obtained at the mooring sites 2 and 3, we use geotriptic winds, computed from 12-hourly atmospheric surface pressure. These surface winds (a balance of Coriolis, pressure gradient, centrifugal, and friction forces) were rotated 15° counterclockwise and reduced in speed by 30% from the geostrophic wind. They were interpolated to a point halfway between moorings 2 and 3 (Fig. 1). Such winds are in good agreement with measured winds at these latitudes (Macklin *et al.,* 1993). The winds at site 1 were strongly influenced by the proximity of the mountainous Alaska Peninsula.

4. Results

a. Ice

The persistent winds (Fig. 2) out of the north during winter of 1994-95 resulted in one of the most extensive ice years in decades. Although the horizontal extent of the ice cover was very large, the ice was thin due to its sudden formation and rapid advection southward. The rapid disappearance of the ice in April supports the inference that, although extensive, the ice was not particularly thick. The presence of first-year ice does not prevent transferral of mixing energy to the water column. Simulations from a model (Overland *et al.,* 1984) designed to investigate the relationships among wind, ice motion, and mixed layer development showed that sufficient turbulence was generated by wind-driven ice to mix the upper 50 m of the water column. This, coupled with tidal mixing, could thus mix the entire water column over the middle shelf.

b. Shipboard measurements

In mid-March, the density structure at mooring 2 consisted of a well-mixed layer capped by a shallow lens of less saline water (Fig. 3a). By late April, the water column exhibited its characteristic structure of two layers separated by a sharp pycnocline at $\sim$37 m. Concentrations of chlorophyll-*a* were low in the late winter. By spring the concentration and distribution of chlorophyll-*a* were similar to previous observations (Sambrotto *et al.,* 1986; Niebauer *et al.,* 1995), with high concentrations of chlorophyll-*a* in the upper layer and relatively low, but nonzero, concentrations in the lower layer.

The concentration of dissolved nitrate was the inverse of the chlorophyll-*a* distribution (Fig. 3b). In March, a high concentration of nitrate occurred from the surface to the bottom

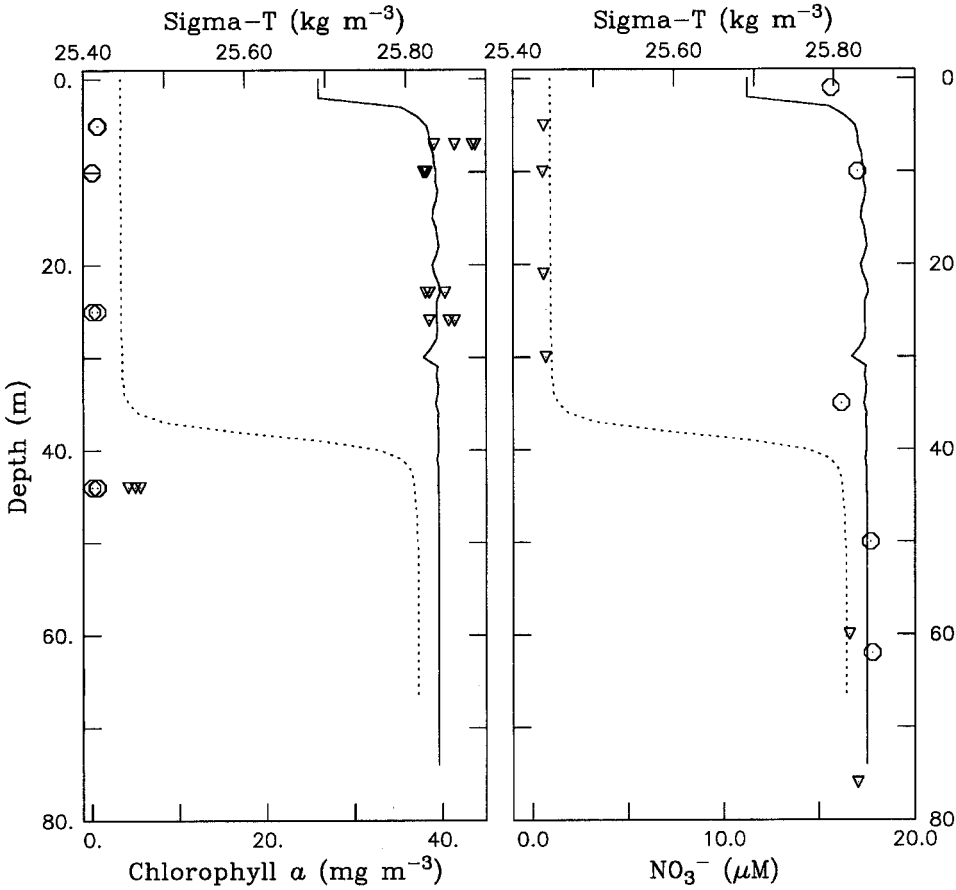

Figure 3. At mooring site 2, (a) concentration of chlorophyll-*a* as measured from CTD casts taken on deployment (circle) and recovery (triangle) and (b) concentration of dissolved nitrate upon deployment (circle) and recovery (triangle). The density structure upon deployment (dashed) and recovery (solid) is also shown in each panel.

of the water column. By April 30, nutrients had been largely depleted from the upper 30 m (the upper mixed layer), but remained high at 60 and 76 m. A week later, nitrate was undetectable in the upper 30 m of the water column.

At mooring site 1 concentrations of dissolved nitrate were high throughout the water column on March 14 and April 23 (Fig. 4). By May 5 a slight draw-down of nutrients had occurred in the upper 20 m. Seven days later on May 12 concentrations of nitrate had been significantly reduced throughout the water column and depleted at the surface. Concentrations of chlorophyll were low or undetectable until May 12.

The structure and properties of the water around mooring 3 differed markedly from those around moorings 1 and 2 (Fig. 4a). On deployment there was a deep (60 m) mixed layer. In spring the remnant of this mixed layer was still evident, with a shallow active mixed layer

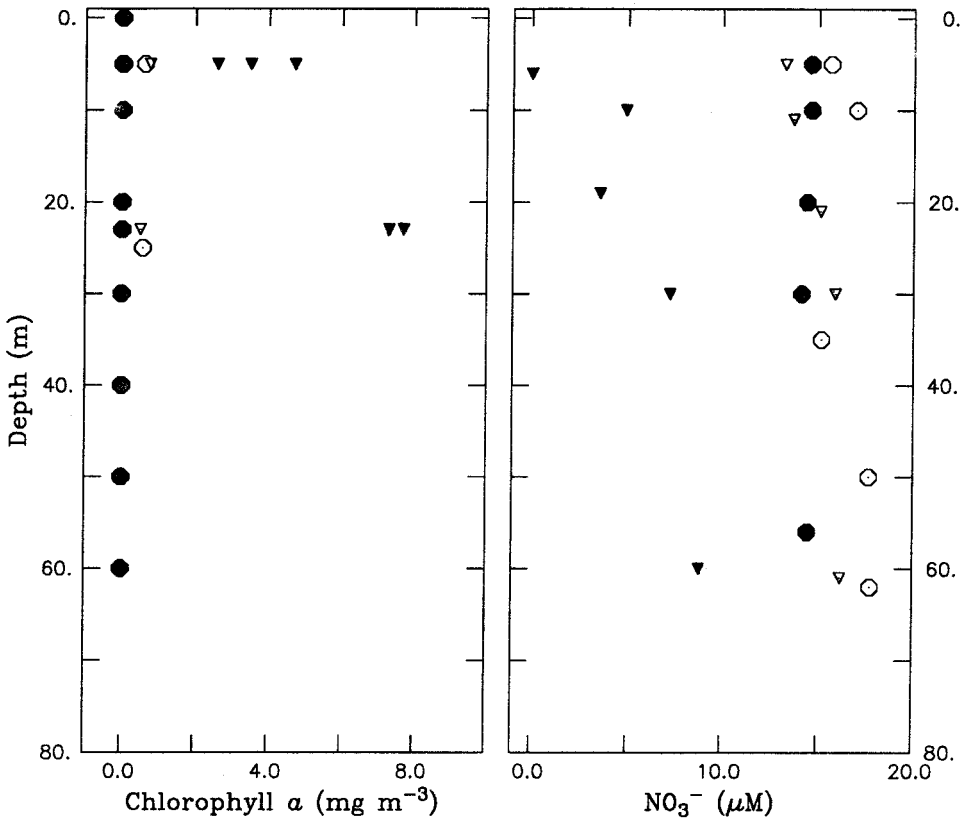

Figure 4. At mooring site 1, (a) concentration of chlorophyll-*a* as measured from CTD casts on March 14 (open circle), April 23 (closed circle), May 5 (open triangle), and May 17 (closed triangle); (b) concentration of dissolved nitrate for same days as in (a).

in the upper $\sim$15 m. In the winter the single chlorophyll measurement at 7 m was low, and in spring a high concentration of chlorophyll occurred uniformly in the upper 45 m. Although maximum concentration was less than measured at mooring 2, concentrations of $>$ 20 mg m^{-3} of chlorophyll occurred deeper in the water column, an effect of the mixed layers at mooring 3 being deeper than at mooring 2.

In March at mooring 3, dissolved inorganic nitrate concentration was uniform in the upper mixed layer (Fig. 4b) and slightly higher at 76 m. In early May, when mooring 3 was recovered, concentration had decreased in the upper layer, but remained high below the pycnocline at 81 m. Unlike at mooring 2, the ice edge bloom did not completely exhaust the nutrients in the upper layer on the outer shelf.

From the chlorophyll-*a* observations it is evident that a phytoplankton bloom occurred at sites 2 and 3 during April, while at site 1 the bloom began much later in mid May. The time-series observations at the moorings permit us to examine the evolution of the early under-ice phytoplankton bloom.

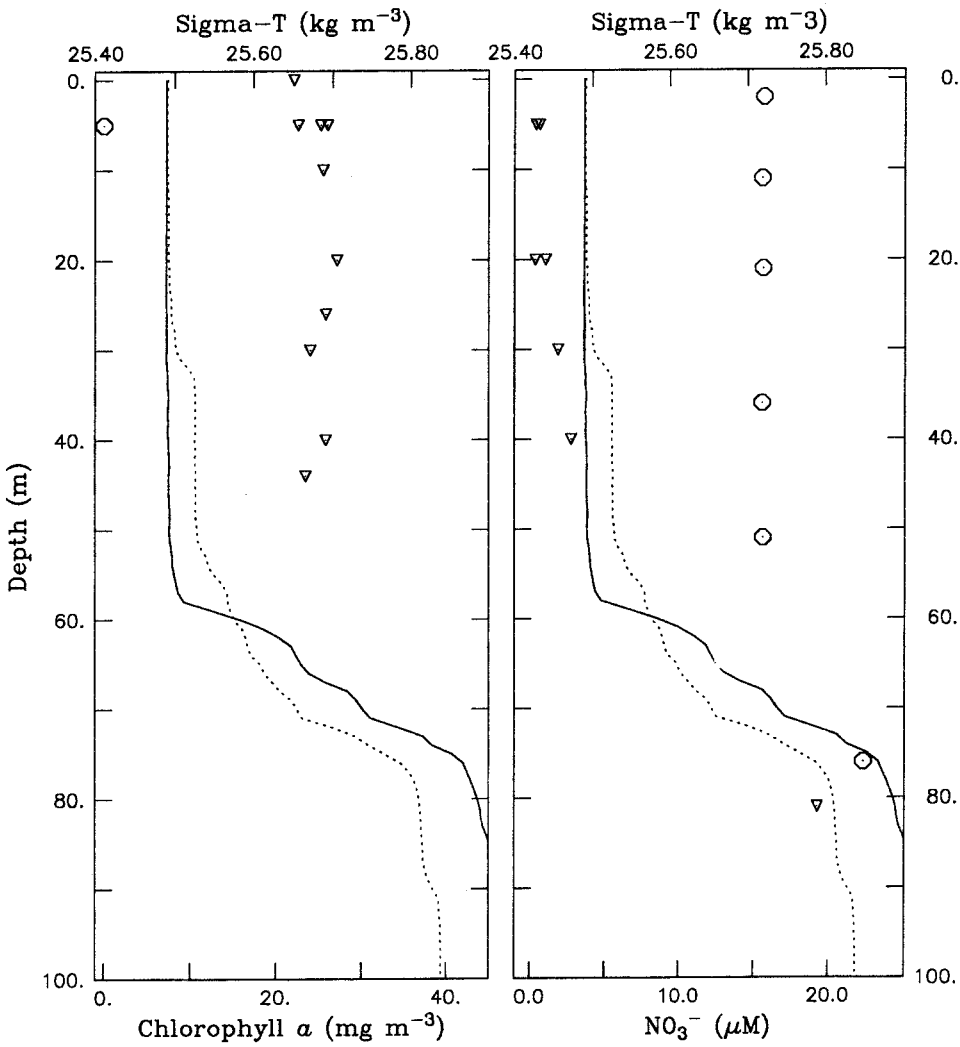

Figure 5. As in Figure 3, except for mooring site 3.

c. Middle Shelf: Mooring 2

Temperature was measured at eight depths on the mooring and at the nearby TRAP (Table 1; Fig. 5a). Initially, wind and tidal mixing resulted in uniform temperature from top to bottom ($\sim$0.5°C). As the ice was blown southward shortly after deployment and melted by the warmer water, the water temperature decreased. On March 27, at its coldest, the water column was isothermal at <-1.5°C. The melting ice decreased initial salinity ($\sim$32.25 psu) by $\sim$0.5 psu at 44 m (Fig. 5b). Although surface salinity likely began decreasing with the arrival and melting of sea ice, the decrease in salinity at this depth resulted from deepening of the mixed layer, which occurred several days after the arrival of

ice. The shallow (<5 m) surface layer evident in the CTD data taken during deployment has been mixed away. At these low temperatures the thermal expansion coefficient of water is small and any change in density is controlled by changes in salinity. Thus, the uniformity in temperature was not due to convective mixing. The energy required for mixing the water column resulted from the four days (beginning March 23) of strong winds (>10.0 m s^{-1}).

To account for the change in temperature, we use a simple box model (Azumaya and Ohtani, 1995). The change in temperature (ΔT) produced by the latent heat from melting ice can be calculated as

$$\Delta T = (Sc - Si)/(Sc - Sb)(Lh/C) \quad (1)$$

where Sc is salinity of the water beneath the ice, Sb is the salinity of the ice, and Si is salinity of water after ice melt. Lh is the latent heat (3.4×10^5 J kg^{-1}) and C the specific heat of the 76-m water column (4.2×10^3 J kg^{-1} °C^{-1}). The salinity measured at the moorings was $Sc = 32.25$ psu before mixing occurred and $Si = 31.8$ psu afterward. Using $Sb = 10.0$ psu, since this is new ice, yields $\Delta T = 1.6$°C, which is consistent with the observed change of temperature form 0.0°C to −1.7°C. If $Sb = 5$ psu, a typical salinity of old ice (Azumaya and Ohtani, 1995), then $\Delta T = 1.3$°C.

From March 30 to April 1, strong currents (∼15 cm s^{-1}) from the southwest resulted in the temperature below ∼25 m rapidly increasing by ∼1.5°C. At this location the two-layer structure was not initiated by freshwater resulting from ice melt, but rather by advection of warmer, more saline water into the lower layer. For the remaining 30 days of this deployment the temperature in the bottom layer (the cold pool) remained relatively constant. The upper layer, however, underwent significant warming starting on April 15, when winds out of the south caused the ice to quickly disappear via melting and/or advection. The warming of the upper layer enhanced the two-layer structure.

The low-frequency currents were not uniform with depth (Fig. 6a). The net speed ranged from 3.7 cm s^{-1} near the surface to 1.0 cm s^{-1} at the bottom. Also evident were pulses of currents >10 cm s^{-1} lasting 2-3 days, which are common over the middle shelf (Schumacher and Kinder, 1983).

Vertical shear was calculated using velocity from the 4-m bins from the ADCP (Fig. 7). The mixed layer depth was defined as the depth at which the temperature differed by 0.1°C from that measured at 1 m. Because of the sparseness of temperature sensors, the depth is only an estimate. There is a close relationship between mixed-layer depth and shear, with maximum shear usually occurring below the mixed layer. There were two periods of large shear. The first coincided with the storm which forced ice southward over the mooring, indicating active mixing during ∼5 days. Enhanced shear is evident to bottom of the water column. The second and largest shear occurred after the establishment of a two-layered system. (Note that the upper layer is not always uniform, but at times is weakly stratified.) From April 8-25, the mixed layer did not deepen below 20 m, even with the presence of strong shear beneath the mixed layer. The storm of April 24-25 deepened the mixed layer

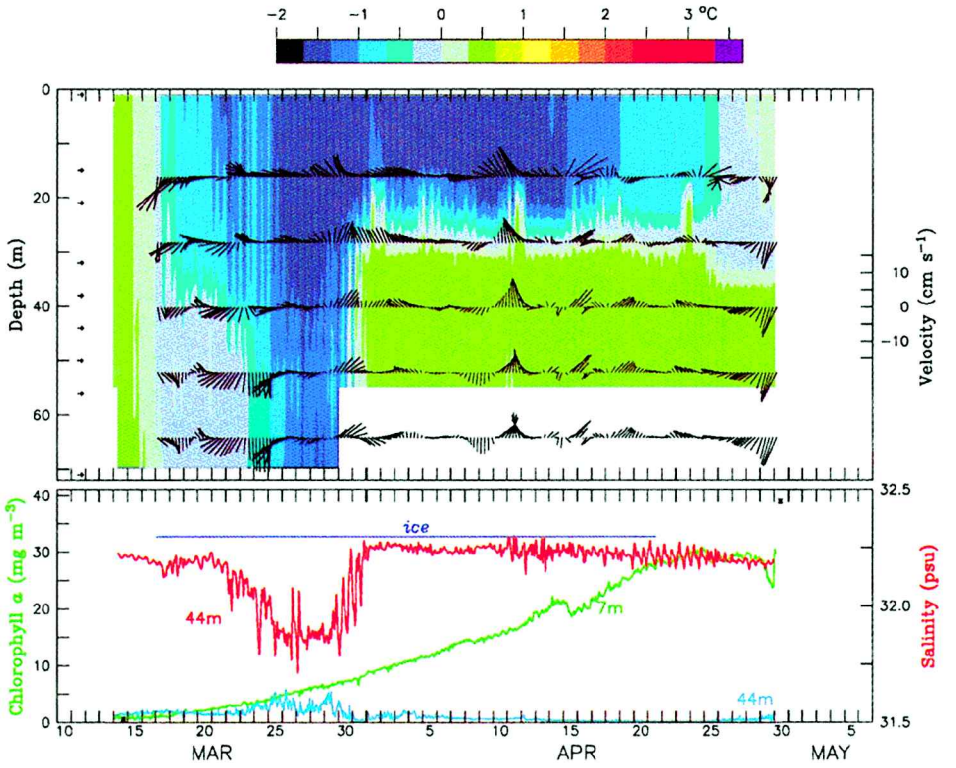

Figure 6. (a) Temperature measured at mooring 2. The vertical location of each instrument is indicated by an arrow along the depth axis. Plotted over the contours of temperature at the appropriate depths are 6 hourly low-pass filtered current vectors (upward indicates northward flow). (b) Chlorophyll-*a* as determined by an A-3 (7 m) and as inferred from a fluorometer (44 m). The estimated period when ice covered the mooring is indicated by the blue line. Salinity at 44 m (the shallowest SEACAT that gave data) is shown in red.

by ~5 m. It is not known whether this change in depth is also related to the removal of the ice, which occurred a few days earlier.

Four days after the arrival of ice and ensuing melting, the chlorophyll-*a* concentration at 7 m began increasing (Fig. 6b). It continued a steady increase of ~0.6 mg m^{-3} d^{-1} until the ice began to retreat, after which the concentration remained relatively constant. The sharp decrease in chlorophyll-*a* on April 15 coincided with a storm which increased the shear beneath ~30 m. The deepening of the upper layer on April 25 also resulted in a slight decrease in chlorophyll-*a*. The concentration of chlorophyll (determined by fluorometry) at 44 m remained low except when the water column actively mixed to below 60 m. The salinity, temperature, and shear all indicate that an active mixing occurred to below 50 m during ~5 days in late March. The chlorophyll at 44 m increased to that observed at 7 m as

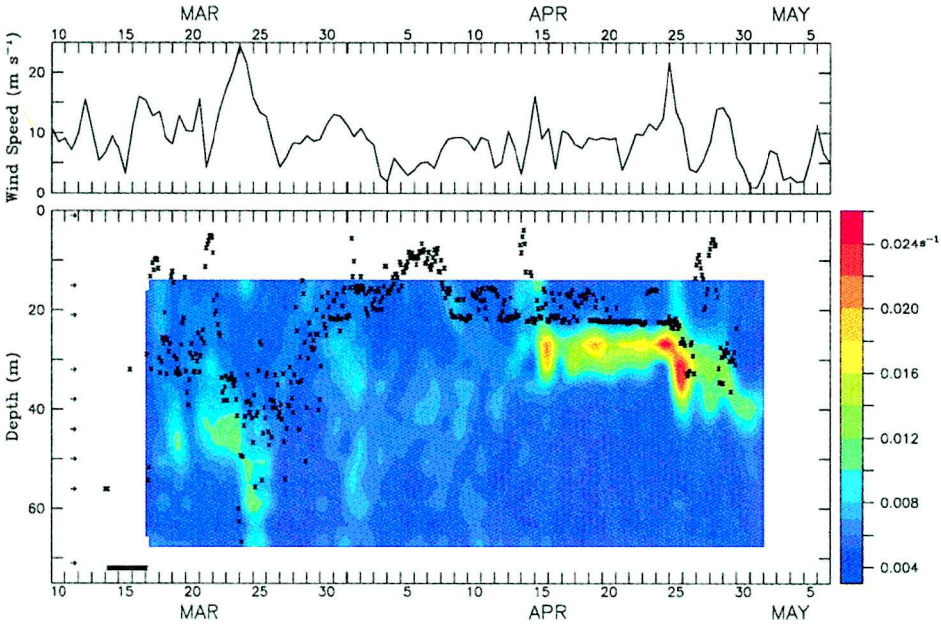

Figure 7. (a) Wind speed derived from atmospheric pressure. (b) Daily averaged shear (s^{-1}) determined from hourly ADCP records at mooring 2. Velocity was measured in 4-m bins. The 2-hourly depth of the mixed layer (defined by differing by 0.1° from the temperature at 1 m) at 6-hr intervals is indicated by +.

a result of the mixing of the water column. It is interesting that the chlorophyll at 7 m continued to increase during this time.

The high-frequency variability evident in both the temperature and chlorophyll-*a* series is tidal in nature (M_2 and K_1 are the dominant tidal constituents at this site) and provide an indication of the horizontal variability in temperature, salinity, and chlorophyll-*a* in the vicinity of mooring 2. The tidal ellipse at mooring 2 was ~5 km in diameter, indicating that the horizontal gradients in the immediate vicinity of the mooring were weak.

d. Outer shelf: Mooring 3

The temperature structure at mooring 3 (Fig. 8a), which was characteristic of the outer shelf, differed markedly from that at mooring 2 (Fig. 6a). A surface mixed layer (60 m) existed over a stratified lower layer. The lowest temperatures occurred with the onset of ice, but were evident only in the upper 40 m. Once again the changes in salinity determined the changes in density. If the newly melted ice is mixed over 45 m, $Sc = 31.9$ psu, $Si = 31.55$ psu, and applying Eq. 1 with $Sb = 10$ psu (5 psu) yields a temperature loss of $\Delta T = 2.2$°C (1.8°C). This compares well with the observed change of temperature from 0.5°C to −1.5°C. Currents at mooring 3 were stronger than those observed at mooring 2, where the

mean flow was very weak. These stronger currents would result in greater advection of water, thus making 1-dimensional models less reliable.

As at mooring 2, the chlorophyll-*a* concentration increased at site 3 upon advent of the ice and accompanying ice melt (Fig. 8b). The maximum concentration, however, was less than observed at mooring 2, and there was also more variability in chlorophyll-*a*. The sharp decreases which occurred at mooring 3 on April 15 and 24-25 also occurred at mooring 2, likely a result of atmospheric forcing which is similar at both stations. The tides once again caused the diurnal variability evident in the time series.

The chlorophyll estimates from water samples were approximately twice those estimated from the moored absorbance meter at mooring 3. A smaller discrepancy occurred at mooring 2. These discrepancies may have resulted from horizontal variability, but more likely resulted from use of an average chlorophyll-specific absorbance coefficient obtained from literature rather than specifically tuned for the types and physiological state of the phytoplankton present at the moorings (Bricaud and Stramski, 1990).

e. Mixed layer depth

Time series of chlorophyll-*a* and mixed layer depth at each mooring (Fig. 9) showed that chlorophyll-*a* concentrations increased during periods of stability. These mixed-layer depths were defined using temperature data. Mixed-layer depths determined from the salinity data at moorings 1 and 3 are consistent with depths determined from temperature. It is interesting that at mooring 1 the stable water column in March did not support a bloom, even though it did at mooring 2.

5. Conclusions

Atmospheric and ice phenomena during the winter and spring of 1994-1995 provided the first time series from moored instruments of chlorophyll-*a*, vertical structure, and currents throughout the water column prior to, during, and after ice retreat. While these measurements were only at single points, they have temporal resolution previously not available. These observations illustrate a sequence of processes leading to an ice-melt phytoplankton bloom and complement previous results from shipboard observations which provide more spatial resolution but limited temporal resolution (Niebauer *et al.,* 1995). The initial cooling from the previous summer's warm ($\sim$10°C) upper-layer water temperatures occurred before the arrival of ice, and resulted from fluxes to the atmosphere.

With cold (<-10°C) winds from the north, ice was blown over the southeastern shelf. The latent heat flux due to ice melt further reduced water temperatures (by $\sim$2.0°C) and also reduced salinity (by $\sim$0.5 psu). Although the latter provided a positive flux of buoyancy, it was not sufficient to prevent mixing. Wind (acting on ice or directly on water) and tidal stirring resulted in near-isothermal conditions over the middle shelf. Over the deeper outer shelf, winds provided the mixing energy to create a shallow ($\sim$30-m) mixed layer.

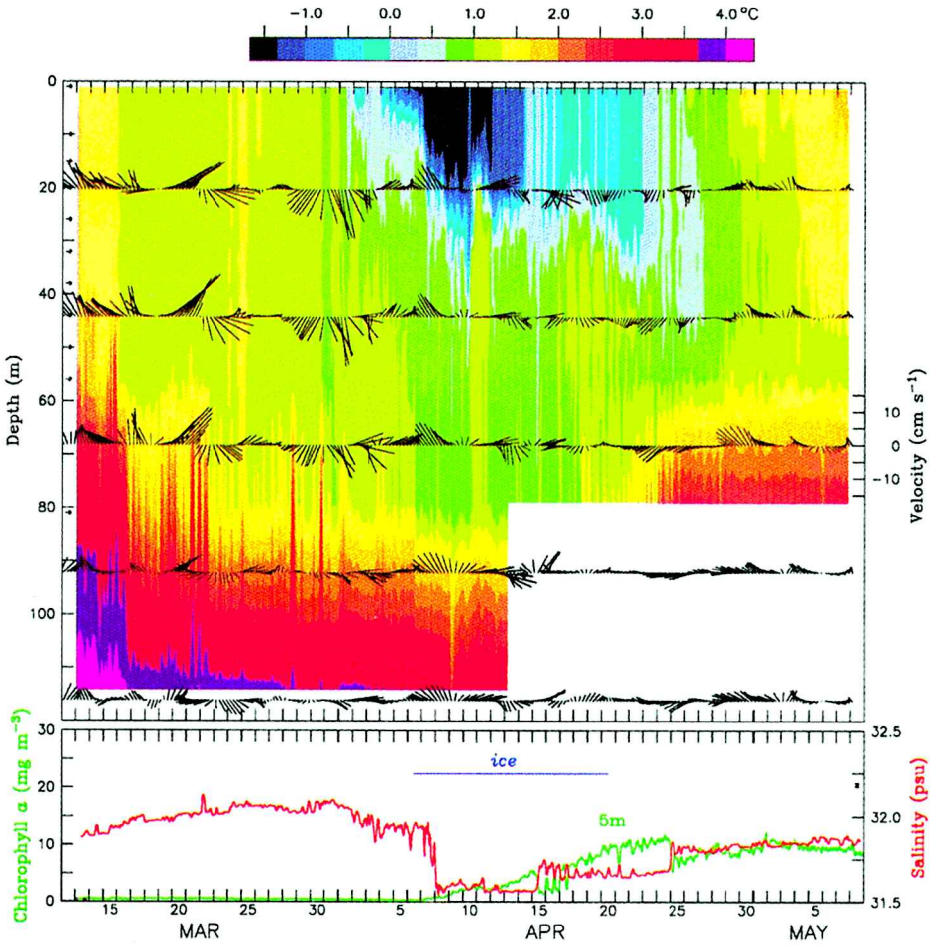

Figure 8. (a) Temperature measured at mooring 3. The vertical locations of the measured temperatures are indicated by arrows. Plotted over the contours of temperature at the appropriate depths are 6 hourly low pass filtered current vectors. (b) chlorophyll-*a* as measured by an A-3 (7 m) is shown in green. The period when ice covered the mooring is indicated by the blue line. Salinity at 10 m is shown in red.

Tidal diffusion has been thought to dominate distribution of water properties over the middle shelf (Coachman, 1986). Our observations, however, show that advection of relatively warm, saline lower-layer water established the vertical structure over the middle shelf. Once instituted, this structure persisted. The ensuing ice melt and warming due to solar radiation enhanced the two-layer structure. Each year, nutrients are lost to the middle shelf and must be replenished by a combination of vertical mixing, release from sediments, nitrification, and horizontal fluxes (Whitledge *et al.,* 1986). During winter (prior to

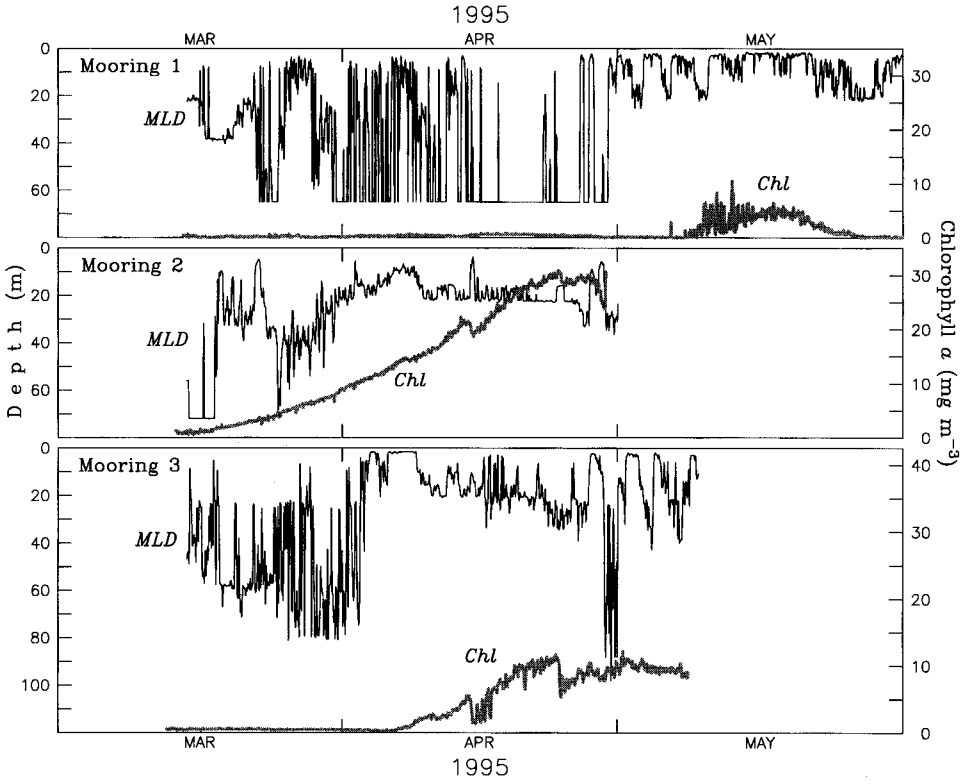

Figure 9. The 2-hourly depth of the mixed layer and hourly concentration of chlorophyll-*a* estimated from A-3 for (a) mooring 1, (b) mooring 2, and (c) mooring 3.

formation of the two layers over the middle shelf), advective events like those observed in these records likely replenish the nutrients on the middle shelf, which are needed for blooms during the following spring. In the past, advection was thought to play no role in the nutrient and salt flux onto the middle shelf. The potential contribution for advection must now be considered as a mechanism for nutrient replenishment.

The high-resolution temporal evolution of an under-ice phytoplankton bloom has not previously been measured. Although the sites were at similar latitudes, the timing of initiation of the phytoplankton bloom and the ensuing chlorophyll maximum differed markedly ($\sim$40 days), corresponding with the presence or absence of melting ice. At mooring 2, over the middle shelf, the steady increase in chlorophyll persisted through a 5-day period when active mixing extended to $>$40 m. Chlorophyll-*a* increased under the ice at both locations. It continued to increase for the duration of the ice cover, leveling off after ice retreat. Levels of chlorophyll-*a* in this study were similar to those at ice algae blooms (23 mg m^{-3}, Alexander and Chapman, 1981) and subsequent ice-edge blooms (Neibauer *et al.,* 1995).

During years of minimal ice cover, a bloom does not begin until mid-April or early May (Sambrotto *et al.,* 1986). During these years the trigger for the bloom is the occurrence of stratification, which allows the phytoplankton growth to exceed respiration loss. The presence of melting ice encourages an earlier bloom. Although chlorophyll-*a* concentrations increased during a short period when the water column was mixing, it is unknown whether this could continue if such conditions persisted.

Acknowledgments. We wish to thank L. Britt, C. DeWitt, D. Dougherty, D. Kachel, L. Long and W. Parker for preparing the equipment and processing data, as well as S. Salo and the crew of the NOAA ship *Miller Freeman* for finding and recovering mooring 2. Special thanks goes to H. Milburn and the engineering group for the excellent design of the moorings, which permitted the gathering of the data presented in this paper. This research was sponsored by NOAA's Bering Sea FOCI Coastal Ocean Program. This is NOAA's Fisheries Oceanography Coordinated Investigations Contribution FOCI-B278 and NOAA's Pacific Marine Environmental Laboratory Contribution 1741.

REFERENCES

Alexander, V. and T. Chapman. 1981. The role of epontic algal communities in Bering Sea ice, *in* The Bering Sea Shelf: Oceanography and Resources, *2,* D. W. Hood and J. A. Calder, eds., U.S. Dept. Commerce, 757–761.

Azumaya, T. and K. Ohtani. 1995. Effect of winter meteorological conditions on the formation of the cold bottom water in the eastern Bering Sea shelf. J. Oceanogr., *51,* 665–680.

Bricaud, A. and D. Stramski. 1990. Spectral absorption coefficients of living phytoplankton and nonalgal biogenous matter: a comparison between the Peru Upwelling area and the Sargasso Sea. Limnol. Oceanogr., *35,* 562–582.

Coachman, L. K. 1986. Circulation, water masses and fluxes on the southeastern Bering Sea shelf. Cont. Shelf. Res., *5,* 23–108.

Cooney, R. T. and K. O. Coyle. 1982. Trophic implications of cross-shelf copepod distributions in the southeastern Bering Sea. Mar. Biol., *70,* 187–196.

Davis, R. F., C. C. Moore, J. R. V. Zaneveld and J. M. Napp. 1997. Reducing the effects of fouling on chlorophyll estimates derived from long-term deployments of optical instruments. J. Geophys. Res., *102,* C3, 5851–5855.

Macklin, S. A., P. J. Stabeno and J. D. Schumacher. 1993. A comparison of gradient and observed over-the-water winds along a mountainous coast. J. Geophys. Res., *98,* 16,555–16,569.

Niebauer, H. J. 1991. Bio-physical oceanographic interactions at the edge of the Arctic ice pack. J. Mar. Sys., *2,* 209–232.

Niebauer, H. J., V. Alexander and S. M. Henrichs. 1995. A time-series study of the spring bloom at the Bering Sea ice edge. I. Physical processes, chlorophyll and nutrient chemistry. Cont. Shelf Res., *15,* 1859–1877.

Overland, J. E., H. O. Mofjeld and C. H. Pease. 1984. Wind-driven ice drift in a shallow sea. J. Geopys. Res., *89* (C4), 6525–6531.

Parsons, T. R., Y. Maita and C. M. Lalli. 1984. A Manual of Chemical and Biological Methods for Seawater Analysis, Pergamon, Toronto, 173 pp.

Sambrotto, R. N., H. J. Niebauer, J. J. Goering and R. L. Iverson. 1986. Relationships among vertical mixing, nitrate uptake, and phytoplankton growth during the spring bloom in the southeast Bering Sea middle shelf. Cont. Shelf. Res., *5,* 161–198.

Schandelmeier, L. and V. Alexander. 1981. An analysis of the influence of ice on spring phytoplankton population structure in the southeast Bering Sea. Limnol. Oceanogr., *26,* 935–943.

Schumacher, J. D. and P. J. Stabeno. 1998. The continental shelf of the Bering Sea, *in* The Sea, Vol. XI—The Global Coastal Ocean: Regional Studies and Synthesis, J. Wiley and Sons, Inc., New York, (in press).

Schumacher, J. D. and T. H. Kinder. 1983. Low-frequency current regimes over the Bering Sea shelf. J. Phys. Oceanogr., *13,* 607–623.

Smith, W. O. 1987. Phytoplankton dynamics in marginal ice zones. Oceanogr. Mar. Biol. Ann. Rev., *25,* 1–38.

Walsh, J. J. and C. P. McRoy. 1986. Ecosystem analysis in the southeastern Bering Sea. Cont. Shelf Res., *5,* 259–288.

Whitledge, T. E., S. C. Malloy, C. J. Patton and C. D. Wirick. 1981. Automated nutrient analysis in seawater. Tech. Rep. BNL-51398, Brookhaven Natl. Lab., Upton, N.Y.

Whitledge, T. E., W. S. Reeburgh and J. J. Walsh. 1986. Seasonal inorganic nitrogen distributions and dynamics in the southeastern Bering Sea. Cont. Shelf. Res., *5,* 109–132.

Wyllie-Echeverria, T. 1995. Seasonal sea ice, the cold pool and Gadid distribution on the Bering Sea shelf. Ph.D. thesis, Univ. of Alaska, Fairbanks, 281 pp.

Received: 19 July, 1996; revised: 15 July, 1997.